HHS Public Access

Author manuscript

Mol Cancer Res. Author manuscript; available in PMC 2018 June 01.

Published in final edited form as:

Mol Cancer Res. 2017 December ; 15(12): 1656–1666. doi:10.1158/1541-7786.MCR-17-0012.

APOPTOTIC BODIES ELICIT GAS6-MEDIATED MIGRATION OF AXL-EXPRESSING TUMOR CELLS

Annelien J.M. Zweemer[1,2], **Cory B. French**[3], **Joshua Mesfin**[2], **Simon Gordonov**[1,2], **Aaron S. Meyer**[1], and **Douglas A. Lauffenburger**[1,2]

[1]Koch Institute for Integrative Cancer Research, Massachusetts Institute of Technology, Cambridge MA 02139, USA

[2]Department of Biological Engineering, Massachusetts Institute of Technology, Cambridge MA 02139, USA

[3]Department of Biomedical Engineering, University of Florida, Gainesville FL 32611, USA

Abstract

Metastases are a major cause of cancer mortality. AXL, a receptor tyrosine kinase (RTK) aberrantly expressed in many tumors, is a potent oncogenic driver of metastatic cell motility and has been identified as broadly relevant in cancer drug resistance. Despite its frequent association with changes in cancer phenotypes, the precise mechanism leading to AXL activation is incompletely understood. In addition to its ligand growth arrest specific-6 (Gas6), activation of AXL requires the lipid moiety phosphatidylserine (PS). PS is only available to mediate AXL activation when it is externalized on cell membranes, an event that occurs during certain physiologic processes such as apoptosis. Here it is reported that exposure of cancer cells to PS-containing vesicles, including synthetic liposomes and apoptotic bodies, contributes to enhanced migration of tumor cells via a PS-Gas6-AXL signaling axis. These findings suggest that anti-cancer treatments that induce fractional cell killing enhance the motility of surviving cells in AXL-expressing tumors, which may explain the widespread role of AXL in limiting therapeutic efficacy.

Introduction

AXL is a member of the TAM (Tyro3, AXL, MerTK)-family of receptor tyrosine kinases (RTKs). Under healthy conditions, TAMs serve a prominent role in regulating the innate immune system [1], but in tumor cells their aberrant expression promotes survival, chemoresistance, and motility [2]. The mechanism of TAM receptor activation is unique among RTK families, requiring both a protein ligand and the lipid moiety phosphatidylserine (PS) [3,4]. In healthy cells, nearly all PS is present on the inner leaflet of the plasma membrane but is externalized on apoptotic cell membranes and apoptotic bodies (ABs) [5,6]. PS exposure allows immune cells that express TAM receptors to engulf these membrane structures. At the same time, TAM activation negatively regulates the innate immune system [1,7,8]. Consistent with these roles, TAM knockout mice exhibit accumulation of PS-positive cell debris in various tissues and autoimmune disorders [9,10]. The role of PS in

Corresponding Authors: Aaron S. Meyer, aameyer@mit.edu, Douglas. A. Lauffenburger, lauffen@mit.edu.

driving TAM-mediated immune cell responses is well established, but the contribution of PS in TAM-mediated cancer signaling remains poorly understood.

In cancer, expression of AXL widely correlates with poor survival and is associated with drug resistance, migration, invasiveness, and metastatic spread [11-14]. RTKs such as EGFR have been reported to transactivate AXL in a ligand-independent manner [15], whereas ligand-dependent activation of AXL is mediated by PS and the bridging ligand Gas6 [16]. γ-carboxylation of the amino terminus of Gas6 is required for its interaction with PS, while the carboxy-terminal domain of Gas6 binds to the AXL ligand-binding domains (Fig. 1A). AXL and Gas6 interact through high-affinity (Ig1) and low-affinity (Ig2) binding interfaces (Fig. 1A). We previously reported the mechanism of this ligand-dependent AXL activation: extracellular vesicles enriched in PS cluster Gas6 ligand, which increases local ligand concentration. This localized concentration promotes binding at the low-affinity site Ig2 of ligands already bound at the high-affinity site Ig1. In conjunction with diffusional transport of unoccupied AXL within the plasma membrane to the sites of localized Gas6 presentation, this asymmetric bi-valent binding process leads to enhanced AXL activation [17]. These findings motivated us to explore the phenotypic consequences of this unique PS-dependent mechanism of receptor activation.

ATP-dependent enzymes called flippases normally keep PS inside the cell, but PS is exposed by the activation of scramblases on the cell surface in biological processes such as apoptosis [18,19]. However, even in non-apoptotic tumor cells, PS can appear on the outer leaflet, which is accompanied by increased shedding of microvesicles [20,21]. In addition, higher rates of apoptosis within the tumor environment, as well as therapy-induced apoptosis, contribute to bursts of PS exposure and release of PS-expressing apoptotic bodies.

Thus, we hypothesized that surviving AXL-expressing tumor cells may take advantage of a resulting PS-mediated increase in local Gas6 ligand concentration, leading to increased AXL activation and the phenotypic alterations of these cells. This may help explain the widely reported role of AXL in cancer therapeutic resistance. In this report we investigate the effect of PS-expressing vesicles on cancer cell behavior. We find that PS/Gas6-dependent AXL signaling promotes cancer cell migration, but does not alter cell proliferation. Our results offer new mechanistic insights into the microenvironmental conditions under which AXL may significantly contribute to cancer cell migration, providing understanding that should help facilitate more effective therapeutic targeting.

Materials and Methods

Reagents

Gas6 was obtained from R&D Systems (Minneapolis, MN). Warfarin was obtained from Santa Cruz Biotechnology (Santa Cruz, CA). R428 was obtained from Fisher Scientific (Pittsburgh, PA). DOPS (1,2-dioleoyl-sn-glycero-3-phospho-L-serine, sodium salt), DOPC (1,2-dioleoyl-sn-glycero-3-phosphocholine), and Coagulant I (DOPE:DOPS:DOPC, 5:3:2 w/w) were obtained as 99% powder from Avanti Polar Lipids, Inc. (Alabaster, AL).

Cell culture

All cell lines were obtained from ATCC. Cells were tested and authenticated according to the cell banks protocol, by assessing short tandem repeat (STR) DNA profiles. Mycoplasma tests were performed in house by using MycoAlert Mycoplasma Detection Kit (Lonza, Walkersville, MD). MDA-MB-231 cells were grown in DMEM, HCC827 in RPMI-1640, and SK-MES-1 in EMEM, all supplemented with 10% FBS and 1% penicillin-streptomycin. Nuclear red MDA-MB-231 and SK-MES-1 cell lines were obtained by transfection with NucLightTM Red Lentivirus Reagent (Essen Bioscience, Ann Arbor, MI) according to the manufacturer protocols.

Generation of AXL knockout cell line using CRISPR/Cas9

An AXL knockout MDA-MB-231-red cell line was generated with the CRISPR/Cas9 system, using plasmid DNA that was kindly provided by the Jaenish lab (MIT). The gRNA sequence TCGCCAAGATGCCAGTCAAG targeting the AXL kinase domain was subcloned in a mammalian expression CRISPR/Cas9 and GFP vector (pSpCas9(BB)-2A-GFP (PX458), Addgene #48138) [22]. Cells were transfected in 6-well plates using 8 μg of plasmid DNA and 20 μL Lipofectamine2000 transfection reagent (Fisher Scientific, Pittsburgh PA) per well in OptiMEM (Life Technologies, Carlsbad, CA) for 5 hrs. 48 hrs after transfection, cells were trypsinized, washed in PBS and resuspended in Odyssey Blocking Buffer (Li-cor Biosciences, Lincoln, NE). Cells were incubated overnight with primary AXL antibody MAB154 (R&D Systems, Minneapolis, MN) followed by secondary antibody anti-mouse Alexa Fluor 647. Finally, cells were sorted for the GFP-positive and AXL-negative population using a BD SORP FACSAria I cell sorter. This AXL negative cell population was cultured for subsequent weeks, and AXL knockout was confirmed using ELISA (described below).

Detection of PS in cell cultures

Cells were seeded overnight in full serum medium at a density of 5×10^3 cells per 96-well and then cultured in serum-free medium in the presence of IncuCute™ Annexin V Green Reagent, a highly selective phosphatidylserine (PS) cyanine fluorescent dye [23]. Cell were cultured for 48 hrs inside an incubator imaging system (IncuCyte, Essen BioScience, Ann Arbor, MI) that allowed images to be automatically acquired and registered using a 10× objective.

Preparation of cell lysates

Cells were seeded sparsely (2×10^5 cells per well) in six-well plates overnight and serum-starved for 4 hrs in serum free medium supplemented with 0.35% bovine serum albumin. Warfarin was continuously present in the cell culture medium throughout the entire culture period to prevent Gas6 γ-carboxylation. After starvation, cells were treated with 100 μg/mL warfarin or 1μM R428 for 24 hrs. Cells were lysed in 50 mM Tris, 10% glycerol, 150 mM NaCl, 1% NP40 at pH 7.5 with cOmplete protease inhibitor (Roche) and phosphatase inhibitor I (Boston Bioproducts). Protein concentration was measured by bicinchoninic acid (BCA) assay following the manufacturer's protocol (Thermo Fisher Scientific, Pittsburgh, PA).

Quantification of receptor abundance and phosphorylation

All ELISA measurements were performed in multiplexed fashion, using individually identifiable beads (BioRad Laboratories, Hercules, CA). Briefly, beads were sedimented for 3 min at 10^4×g then resuspended in 80 μL of 100 mM NaH_2PO_4 pH 6.3. 10 μL of 50 mg/mL S-NHS (Invitrogen, Chicago, IL) and 10 μL of 50 mg/mL EDC were added, and the mixture was incubated with agitation for 20 min at room temperature. Beads were then pelleted and resuspended in 300 μL 50 mM HEPES pH 7.4 with 0.1 mg/mL of either AXL, Tyro3, MerTK or Gas6 capture antibody (R&D Systems, Minneapolis, MN). The mixture was incubated overnight at 4°C with agitation. The next day, the beads were washed repeatedly and stored in 1% bovine serum albumin (BSA) in PBS. Coupling efficiency was measured using biotinylated protein G.

Lysates were incubated with capture beads overnight at 4°C with agitation, then washed with 0.1% Tween-20 in PBS and incubated with either detection antibodies for AXL/Tyro3/MerTK/Gas6 (R&D Systems, Minneapolis, MN) or biotinylated anti-phosphotyrosine antibody 4G10 (Millipore Corp, Billerica, MA) for 1 hr. After a second wash, beads were incubated with streptavidin-phycoerythrin (BioRad Laboratories, Hercules, CA) for 10 min and then quantified using a FlexMap 3D (Luminex Corp). AXL and Gas6 abundance was quantified by comparison to a recombinant standard (R&D Systems, Minneapolis, MN).

Preparation of cell debris and isolation of apoptotic bodies

HCC827 cells were seeded in 5-cm plates at a density of 2.5 ×10^6 cells per plate and grown for 24 hrs. After removal of the medium and a wash with PBS, cells were UVC-irradiated (254 nm) using a dose of 5 J/cm^2 with an UVGL-58 handheld UV lamp (UVP, Upland, CA). 4 mL serum free medium with 0.35% BSA was added and cell debris was collected after 24 hrs. Cells were sedimented for 10 min at 300×g and the remaining cell debris mixture was used for assays. To isolate apoptotic bodies, the mixture was centrifuged for an additional 20 min at 16500×g using a Sorvall RC 6 Plus superspeed centrifuge equipped with the Sorvall SS-34 fixed-angle rotor (Thermo Fisher Scientific, Waltham, MA) [24]. Dynamic light scattering (DLS) measurements were performed with a DynaPro NanoStar (Wyatt Technology Corp, Santa Barbara, CA) to determine the distribution and size of the vesicles.

Preparation of liposomes

Lipids were stored as powder under argon at −20°C prior to use. Powders were hydrated with PBS to total lipid concentrations of about 2.0 mg/mL. Multilamellar vesicles (MLVs) were formed through 5 min of high-speed physical agitation with a vortex mixer. Sonicated unilamellar vesicles (SUV) were subsequently prepared from MLV solution through additional pulse sonication for 10 min (10 sec on/10 sec off) with a Branson SLPe probe-tip sonicator (Branson Ultrasonics, Danbury, CT) at 45% maximum power. MLV and SUV solutions were passed through sterile hydrophilic 0.45 μm CA and 0.22 μm PVDF filters, respectively. Liposomes were used in cell culture immediately following synthesis and analyzed for size and distribution by DLS.

Cell proliferation assay

Cell proliferation was evaluated using the CellTiter-Glo Luminescent Cell Viability Assay (Promega, Madison, WI). Cells were seeded overnight in full serum medium at a density of 1×10^3 cells per 96-well, and then cultured in serum-free medium in the presence or absence of inhibitors, liposomes, cell debris and apoptotic bodies for 72 hrs. For knockdown, cells were transfected with 25 nM of nontargeting siRNA or siRNA targeting AXL using DharmaFECT 1 (SK-MES-1) or DharmaFECT 4 (MDA-MB-231) transfection reagent (GE Dharmacon, Lafayette, CO), according to the manufacturer's instructions. All further analysis was performed 72 hrs after siRNA transfection.

Wound confluence assay

Cells were plated at a density of 4.5×10^4 cells per well in an uncoated 96-well Essen ImageLock plate, allowed to grow overnight in full serum (10% FBS) medium, and then loaded into the 96-pin WoundMaker device (Essen BioScience, Ann Arbor, MI). After scratching, wells were washed twice with PBS to prevent settling and reattachment of dislodged cells. Next, serum-free medium with or without inhibitors, liposomes or cell debris was added and the plate was placed inside an incubator imaging system (IncuCyte, Essen BioScience). Wound images were automatically acquired and registered by the IncuCyte™ software system. Data of unlabeled cells are presented as the Relative Wound Density (RWD, Eizen, v1.0 algorithm). RWD is a representation of the cell density (per unit area) in the established wound area relative to the cell density outside of the wound area at the corresponding time point (time-curve). Wound-closure images of cells labeled with a red nuclear reporter were analyzed using custom scripts written in MATLAB (MathWorks, Natick, MA). The image processing and quantification workflow for cell migration analysis is presented in Fig. S2. Briefly, wound boundaries were identified through summation of fluorescence intensities of nuclei along the direction parallel to the direction of the wound. K-means clustering of the sums was used to partition the image into low-intensity and high-intensity groups that correspond to areas inside and outside the wound. Wound edges were defined as the locations of change from the high- to low-intensity cluster. Locations of individual cell nuclei were identified via detection of point sources of fluorescence in each image. Migration data are presented as the wound closure rate (WCR), where the WCR is the average rate of change of RWD in the first 24-hours following scratch of the culture.

Results

PS-Gas6 mediated AXL activation enhances cancer cell migration

To investigate the phenotypic cellular response of AXL signaling mediated by PS-Gas6, we first identified cell lines that are strongly affected by PS-mediated AXL activation due to autocrine Gas6/PS production. We inhibited AXL signaling using the tyrosine kinase inhibitor R428 or warfarin (Fig. 1A). Warfarin prevents synthesis of vitamin K and thus γ-carboxylation of Gas6, thereby preventing its interaction with PS. R428 inhibits AXL in a ligand independent manner, therefore perturbing the AXL signaling pathway in a different manner compared to warfarin.

The use of both agents enabled us to identify the specific contribution of PS to AXL-mediated signaling. Examining a panel of nine triple-negative breast cancer (TNBC) and non-small cell lung cancer (NSCLC) cell lines (Supplementary Fig. S1A), the TNBC cell line MDA-MB-231 and NSCLC cell line SK-MES-1 exhibited great reliance of AXL activation on PS-Gas6-mediated signaling (Fig. 1B). AXL phosphorylation decreased upon addition of R428 as well as warfarin, the effects of the latter specifically implicating the role of autocrine PS-mediated signaling in AXL activation.

To confirm the presence of exposed PS on MDA-MB-231 and SK-MES-1 cells in culture, we performed an Annexin V binding assay [23]. In this assay, a polarity-sensitive annexin-based biosensor with switchable fluorescence states emits green fluorescence when bound to PS on apoptotic cells. As shown in Fig. 1C, PS-presenting cells and vesicles were identified in the populations of both cell types, confirming the availability of this lipid to activate AXL.

Although both R428 and warfarin inhibited AXL activation, they appeared to do so by distinct effects on cellular signaling and/or trafficking processes. This was indicated by analysis of the AXL expression levels, which were increased in both cell lines upon warfarin stimulation but not upon addition of R428 (Fig. 1B). Similarly, autocrine Gas6 levels were only increased in the presence of warfarin (Fig. 1B).

The two inhibitors also produced different cell proliferation responses. Inhibition of the AXL tyrosine kinase domain by R428 decreased cell proliferation profoundly in MDA-MB-231 and SK-MES-1 cells (Fig. 1D). The role of AXL in this response was confirmed with AXL siRNA treatment, which inhibited proliferation to a similar extent as with R428 treatment in these cell lines (Supplementary Fig. S1B+C). On the other hand, disruption of the Gas6-PS interaction by warfarin did not affect cell proliferation, implying that PS-mediated, ligand-dependent AXL signaling may not contribute to cell proliferation (Fig. 1D).

In contrast to cell proliferation, AXL-mediated cell migration was inhibited to a similar extent by R428 and warfarin in both cell lines (Fig. 1E). Endogenous ligand was sufficient, as exogenous Gas6 did not increase migration rates beyond that driven by the endogenous ligand. Both cell lines did not express Tyro3 and MerTK, the two other TAM family receptors that are activated by PS/Gas6, as determined by ELISA. This further supports that the warfarin-induced decrease in migration resulted from PS-Gas6-AXL inhibition. In total, these data demonstrate that ligand-dependent, PS-mediated AXL activation contributes to the migration of MDA-MB-231 and SK-MES-1 cells, but is not required for cell proliferation.

Apoptotic cell debris induces AXL-mediated cell migration

Our data indicate that AXL-mediated cell migration is driven via Gas6- and PS-dependent activation. PS is usually present on the inner leaflet of cell membranes, but can be exposed when cells undergo apoptosis [18]. Therefore, we hypothesized that AXL signaling may be directly upregulated in an apoptotic environment through PS exposure. This would potentially explain previous observations of AXL-mediated, chemotherapy-induced migration and invasion [25].

To test this hypothesis we performed wound scratch migration assays with MDA-MB-231 cells displaying a live-cell fluorescent nuclear reporter (MDA-MB-231-red cells) in the presence of PS-containing cell debris. The image processing and analysis workflow used to quantify motility of cells labeled with the red nuclear reporter in the wound assay is shown in Supplementary Fig. S2. We induced apoptosis in the AXL-negative tumor cell line HCC827 (no detectable AXL levels by ELISA, data not shown) by UV-irradiation. Cells were removed from the culture medium by centrifugation, resulting in a cell debris mixture containing the soluble secretome as well as apoptotic bodies (Fig. 2A). Treatment of MDA-MB-231-red cells with apoptotic cell debris significantly increased their migratory rate (Fig. 2B/C). This was mediated by factors resulting from apoptosis, since migration was not affected by addition of supernatant from non-UV irradiated HCC827 cells (Supplementary Fig. S3A). Treatment with R428 or warfarin inhibited the debris-induced migration in all cases, suggesting the role of AXL in this process (Fig. 2C). Nevertheless, in several experiments there was a significant increase in migration when comparing inhibitor alone to the combination of inhibitor and cell debris. This suggests that besides PS/Gas6, additional factors present in cell debris mixtures may contribute to cell migration.

Apoptotic bodies induce AXL-mediated cell migration

In order to identify the contribution of the PS-presenting vesicles to cell motility within the cell debris mixture, we first isolated apoptotic bodies (ABs) by centrifugation (Fig. 2A). Addition of isolated ABs increased cell migration to a similar degree as the presence of total cell debris (Fig. 3A). In contrast, the soluble apoptotic secretome did not induce cell migration (Supplementary Fig. S3B), which confirms that the observed increase in cell migration within the UV-treated supernatant fraction was due to addition of apoptotic bodies. Inhibiting AXL with either R428 or warfarin decreased the AB-induced cell migration (Fig. 3A), implicating the role of AXL and PS in this process. Stimulating cells with ABs did not affect cell proliferation (Supplementary Fig. S3C), which is in line with the lack of effect of PS-mediated AXL signaling on cell proliferation as ascertained previously (Fig. 1D).

To confirm the contribution of AXL in the apoptosis-induced migration we repeated experiments with an AXL knockout (KO) MDA-MB-231-red cell line. AXL knockout was obtained using the CRISPR/Cas9 technology [22] and confirmed with ELISA (Supplementary Fig. S4A). R428 and warfarin did not affect cell migration in the MDA-MB-231-red AXL KO cell line (Fig. 3B+C), confirming that the effects of these inhibitors in all previous experiments were exerted via the AXL receptor. AXL knockout reduced the wound closure rate compared to parental MDA-MB-231-red cells (Fig. 3D), in an order of magnitude similar as for treatment with the AXL inhibitors R428 and warfarin (Fig. 3B). Next, we compared the migration of parental and AXL KO cells in the presence of apoptotic bodies, as presented in Fig. 3E. A significant decrease in migration was observed upon addition of apoptotic bodies to the AXL KO cell line compared to the parental cell line, providing evidence that AXL signaling is contributing to apoptosis-induced migration. In the AXL KO cell line a small but significant increase of migration upon addition of ABs remained compared to control (Supplementary Fig. S4B+C), which suggests that additional factors are involved in this process.

PS-containing liposomes induce AXL/Gas6-mediated cell migration

To confirm and validate the contribution of PS to the increased migration response, we made use of synthetic liposomes of varying size and composition (Fig. 4A). Multilamellar (MLVs) and sonicated unilamellar vesicles (SUVs) (Fig. 4B) were synthesized with a 5:3:2 w/w blend of DOPE (1,2-dioleoyl-sn-glycero-3-phosphoethanolamine), DOPS (1,2-dioleoyl-sn-glycero-3-phospho-L-serine), and DOPC (1,2-dioleoyl-sn-glycero-3-phosphocholine) to yield liposome populations of individual vesicles with the blended lipid composition. The 5:3:2 w/w blend approximately represented cell plasma membrane composition after scramblase activation and was therefore selected as appropriate surrogate to mimic apoptotic bodies [26]. The SUV and MLV preparations had distinct average hydrodynamic diameters (D_h) that represent distinct populations comprising sizes germane to the apoptotic cell debris (Fig. 4A). Treatment of MDA-MB-231-red cells with MLV and SUV samples of the lipid blend produced significant pro-migratory responses with a dependence on liposome diameter and a biphasic dose-response relationship (Fig. 4C). Consistent with our previous work [17], this biphasic behavior reflects one of the unique features of lipid-ligand induced AXL activation, and points to changes in AXL localization giving rise to the effect of the Gas6-PS interaction rather than a conformational change due to PS interaction itself. This behavior is schematically presented in Fig. 4D: in the absence of lipid, Gas6 will occupy the high affinity AXL binding domain Ig1, but the low-affinity site Ig2 remains insufficient for receptor dimerization and activation by Gas6. On the other hand, at very high concentrations of lipid, the overabundance of PS prevents the occurrence of high local Gas6-AXL concentrations that are required for AXL dimerization and activation. The latter only efficiently occurs for an optimal ratio of Gas6 and lipids expressing PS.

In order to parse the effects of lipid component composition, SUVs were synthesized with component compositions of DOPS alone, DOPC alone and a 5:3:2 w/w blend of DOPE:DOPS:DOPC (lipid blend). Treatment of MDA-MB-231 cells with SUV compositional variants at a total lipid concentration of 50 μg/mL resulted in increased cell migration only when liposomes contained PS (Fig. 5A). The increase in cell migration with DOPS was similar to that induced by stimulation with EGF, a known pro-migratory stimulus for this cell line (Supplementary Fig. S5A). As with the AB mixtures, cell proliferation was not affected by any of the PS-containing vesicles (Supplementary Fig. S5B).

Treatment with R428 prevented the SUV-induced migration response and inhibited cellular migration under all conditions (Fig. 5A). The combination of warfarin and the SUV compositional variants likewise abolished the increase in migration observed for liposomes containing PS (Fig. 5A). Nevertheless, stimulating warfarin-treated MDA-MB-231 cells with PS liposomes resulted in a small but significant increase in migration compared to warfarin-only treated cells. We hypothesized that this might be the result of residual γ-carboxylated Gas6 in the cell culture medium due to high autocrine Gas6 levels in this cell line (Fig. 1B). To test this, we repeated these experiments for the other cell line, SK-MES-1, which secrete substantially lower levels of autocrine Gas6 compared to MDA-MB-231 cells.

In accordance with the effects on MDA-MB-231 cells, treatment of SK-MES-1 cells with SUV compositional variants increased cell migration only when liposomes contained PS (Fig. 5B). Combination treatment of SUVs and AXL inhibitor R428 or warfarin eliminated

the pro-migratory response and inhibited cellular migration under all conditions (Fig. 5B). In contrast to MDA-MB-231 cells, stimulating warfarin-treated SK-MES-1 cells with PS liposomes resulted in equal migration rates compared to warfarin-only treated cells, potentially due to lower autocrine Gas6 levels.

These results indicate that migration of the cell lines tested is mediated by PS-containing liposomes through AXL activation. The localization of the protein ligand Gas6 by PS in vesicle presentation, either by synthetic liposomes or apoptotic bodies, is essential for this pro-migratory response.

Discussion

This study contributes to our expanding knowledge of the important roles that extracellular vesicles play in cancer cell signaling and function. We introduce the concept of apoptosis-induced migration by demonstrating that phosphatidylserine(PS)-containing vesicles, including apoptotic bodies, enhance cell migration via the AXL receptor (Fig. 6). Elucidating this mechanism of AXL activation is of great importance for designing therapeutic regimens that include AXL targeting by identifying where and when AXL is active.

The involvement of AXL in cancer metastasis has been extensively reported. AXL-mediated downstream signaling events resulting in cell migration have been heavily studied [12,27,28], but the AXL activation mechanism responsible for this phenotype has been largely unknown. Localized Gas6 that is bound to PS on extracellular vesicles was previously reported to mediate ligand-dependent AXL activation [17], and the present study demonstrates that this lipid-ligand-induced AXL signaling enhances cell motility. Warfarin, clinically used as an anti-coagulant [29], prevents binding of *in situ*-produced PS and has been shown to have anti-metastatic effects [30,31]. Similarly, PS-targeting antibodies have been reported to decrease *in vivo* tumor growth [32]. Collectively, these data suggest that the participation of the lipid component PS should be incorporated when investigating the role of AXL in cancer progression.

The concept of apoptosis-induced migration described in this study implies a potential selective advantage of AXL-expressing tumor cells to migrate out of the primary tumor environment and disseminate. Results from Gjerdrum *et al.* provide indications of this phenomenon, having reported that matched patient metastatic lesions exhibit higher AXL levels compared to those in the primary tumor [11]. In addition, it has been demonstrated that chemotherapy-induced migration and invasion of colorectal cancer cells is regulated by AXL [25].

An increasing number of studies report signaling by extracellular vesicles as a major contributor to multiple hallmarks of cancer [33]. While most of these reports focus on the uptake of cargo such as proteins, RNA and DNA carried by these vesicles [34,35], the work presented here provides evidence for direct signaling initiated by the lipid bilayer component PS. This is highly relevant to cancer biology since PS is abundant within the tumor microenvironment, as disrupted membrane asymmetry in tumor cells results in PS exposure

on the outer leaflet of the cell membrane. AXL knockout partly reduced apoptosis-induced cell migration, hence we conclude that other signaling molecules present on/in apoptotic bodies can induce cancer cell migration. In addition, PS acts as a lipid messenger for several other receptors, which may equally be involved in this process [36,37]. Elucidation of these factors remains a subject for future studies.

In this study we identified apoptotic bodies as extracellular vesicles responsible for initiating increased cell motility, since isolation of smaller vesicles such as exosomes would require additional centrifugal force [24]. However, tumor derived exosomes have been reported to express PS in ovarian cancer [20,38]. Since exosomes fall within the size range of the SUV liposomes used in this study (Fig. 4A), we speculate that besides apoptotic bodies, tumor-derived exosomes might also be capable of inducing AXL-mediated cell migration. Irrespective of the type of extracellular vesicles, high levels of PS exposure have been reported to correlate with increased malignant potential of tumor cells [21].

Therapeutic killing of tumor cells results in apoptotic cells that break down into apoptotic bodies, which are highly enriched in PS. Apoptosis was initially regarded as a ‘clean and silent’ mechanism of cell death aimed at eliminating cells by the immune system. Studies in both developmental and cancer biology have revealed the signaling capacities of apoptotic cells affecting neighboring cells, resulting in tissue remodeling, cell proliferation, tumor growth, angiogenesis, and drug resistance [39-43]. Our study adds PS-AXL-induced migration to the list of the paradoxical oncogenic properties of apoptotic cells. Interestingly, our findings revealed that the PS-Gas6-AXL-mediated response does not affect cell proliferation. For that reason, one interpretation of this work is that apoptosis-mediated activation of AXL is part of a migratory cancer cell’s ‘fight or flight’ response during therapy, in which AXL either contributes to the development of drug resistance and/or the enhancement of metastatic capacity.

The mechanistic insight into AXL-mediated migration gained from this work may help to advance the design of more effective therapeutic strategies. AXL is regarded as a promising target for addressing drug resistance and metastasis, and inhibitors for all components of the AXL signaling complex have been developed so far. These modulators include small molecule AXL kinase domain inhibitors [14,44,45], an AXL ‘decoy receptor’ that binds Gas6 in order to inhibit its function [46], and PS-targeting antibodies [32]. Our results indicate that drugs targeting both AXL and Gas6 inhibit cell migration *in vitro*. However, only the small molecule AXL inhibitor R428 decreased cell viability, potentially through inhibition of transactivation of other RTKs [15,47]. For that reason, small molecule AXL kinase inhibitors could provide an additional treatment benefit by inhibiting cell proliferation and drug resistance. We argue that high AXL expression levels in the primary tumor should not necessarily be the selection criteria for patients that would benefit from AXL-targeting drugs. A small subpopulation of AXL-expressing cells within the primary tumor could be sufficient to form metastases by taking advantage of an apoptotic environment produced by fractional cell killing following therapy [11]. This further implies that AXL-targeting agents should be administered simultaneously or prior to other chemotherapeutics in order to diminish the potential for apoptosis-mediated migration through AXL signaling.

One of the open questions raised by the present study is how apoptosis-mediated AXL signaling will manifest in a tumor environment containing immune cells and cancer cells that both express AXL [48], as well as the other TAM-family receptors MerTK and Tyro3, which are also activated by PS and Gas6. Binding of apoptotic bodies to AXL-expressing tumor cells may not only induce migration, but also cause juxtacrine signaling upon interaction with TAM-expressing immune cells to block immunosurveillance [2,31,49]. The escape from immune detection may contribute to metastatic dissemination, and may promote the outgrowth of drug resistant tumor cells. The specific role of PS-Gas6-AXL mediated signaling in the development and maintenance of drug resistance remains to be elucidated.

In summary we have identified novel signaling capacities of extracellular vesicles presenting PS in the context of cancer biology. The concept of apoptosis-induced migration may apply to a wide range of solid tumors expressing AXL, and provides a rationale for including AXL-inhibitors in combinatorial therapies at the onset of cancer treatments to hinder metastatic disease progression.

Supplementary Material

Refer to Web version on PubMed Central for supplementary material.

Acknowledgments

The authors like to thank Dr. Julien Maffat and Atya Omer for providing us with CRISPR/Cas9 plasmid DNA targeting the AXL receptor, as well as their help in troubleshooting the protocol. We thank the Koch Institute Flow Cytometry Core for assistance during flow sorting.

Financial Support

Funding: This work was funded in part by a grant of Merrimack Pharmaceuticals (to DAL), along with NIH R01-CA 96504 (to DAL), DP5-OD019815 (to ASM), and the Koch Institute Support (core) grant P30-CA14051 from the NCI. AJMZ was supported by Ludwig Center for Molecular Oncology Fund. CBF was supported by the University of Florida Science for Life Program.

List of abbreviations

AB	apoptotic body
D_h	hydrodynamic diameter
DLS	dynamic light scattering
DOPC	1,2-dioleoyl-sn-glycero-3-phosphocholine
DOPE	1,2-dioleoyl-sn-glycero-3-phosphoethanolamine
DOPS	1,2-dioleoyl-sn-glycero-3-phospho-L-serine
Gas6	growth arrest specific-6
KO	knockout
MLV	multilamellar vesicle

NS	not significant
NSCLC	non-small cell lung cancer
PS	phosphatidylserine
RTK	receptor tyrosine kinase
RWD	relative wound density
SUV	small unilamellar vesicle
TAM	Tyro3, AXL, MerTK
TNBC	triple-negative breast cancer
WCR	wound closure rate

References

1. Lemke G, Rothlin CV. Immunobiology of the TAM receptors. Nat Rev Immunol. 2008; 8:327–36. [PubMed: 18421305]
2. Graham DK, DeRyckere D, Davies KD, Earp HS. The TAM family: phosphatidylserine sensing receptor tyrosine kinases gone awry in cancer. Nat Rev Cancer. 2014; 14:769–85. [PubMed: 25568918]
3. Stitt TN, Conn G, Gore M, Lai C, Bruno J, Radziejewski C, et al. The anticoagulation factor protein S and its relative, Gas6, are ligands for the Tyro 3/Axl family of receptor tyrosine kinases. Cell. 1995; 80:661–70. [PubMed: 7867073]
4. Varnum BC, Young C, Elliott G, Garcia A, Bartley TD, Fridell YW, et al. Axl receptor tyrosine kinase stimulated by the vitamin K-dependent protein encoded by growth-arrest-specific gene 6. Nature. 1995; 373:623–6. [PubMed: 7854420]
5. Eken C, Martin PJ, Sadallah S, Treves S, Schaller M, Schifferli JA. Ectosomes released by polymorphonuclear neutrophils induce a MerTK-dependent anti-inflammatory pathway in macrophages. J Biol Chem. 2010; 285:39914–21. [PubMed: 20959443]
6. Scott RS, McMahon EJ, Pop SM, Reap EA, Caricchio R, Cohen PL, et al. Phagocytosis and clearance of apoptotic cells is mediated by MER. Nature. 2001; 411:207–11. [PubMed: 11346799]
7. Carrera Silva EA, Chan PY, Joannas L, Errasti AE, Gagliani N, Bosurgi L, et al. T cell-derived protein S engages TAM receptor signaling in dendritic cells to control the magnitude of the immune response. Immunity. 2013; 39:160–70. [PubMed: 23850380]
8. Rothlin CV, Ghosh S, Zuniga EI, Oldstone MB, Lemke G. TAM receptors are pleiotropic inhibitors of the innate immune response. Cell. 2007; 131:1124–36. [PubMed: 18083102]
9. Fourgeaud L, Través PG, Tufail Y, Leal-Bailey H, Lew ED, Burrola PG, et al. TAM receptors regulate multiple features of microglial physiology. Nature. 2016; 532:240–4. [PubMed: 27049947]
10. Seitz HM, Camenisch TD, Lemke G, Earp HS, Matsushima GK. Macrophages and dendritic cells use different Axl/Mertk/Tyro3 receptors in clearance of apoptotic cells. J Immunol. 2007; 178:5635–42. [PubMed: 17442946]
11. Gjerdrum C, Tiron C, Høiby T, Stefansson I, Haugen H, Sandal T, et al. Axl is an essential epithelial-to-mesenchymal transition-induced regulator of breast cancer metastasis and patient survival. Proc Natl Acad Sci U S A. 2010; 107:1124–9. [PubMed: 20080645]
12. Vuoriluoto K, Haugen H, Kiviluoto S, Mpindi JP, Nevo J, Gjerdrum C, et al. Vimentin regulates EMT induction by Slug and oncogenic H-Ras and migration by governing Axl expression in breast cancer. Oncogene. 2011; 30:1436–48. [PubMed: 21057535]
13. Li Y, Ye X, Tan C, Hongo JA, Zha J, Liu J, et al. Axl as a potential therapeutic target in cancer: role of Axl in tumor growth, metastasis and angiogenesis. Oncogene. 2009; 28:3442–55. [PubMed: 19633687]

14. Holland SJ, Pan A, Franci C, Hu Y, Chang B, Li W, et al. R428, a selective small molecule inhibitor of Axl kinase, blocks tumor spread and prolongs survival in models of metastatic breast cancer. Cancer Res. 2010; 70:1544–54. [PubMed: 20145120]
15. Meyer AS, Miller MA, Gertler FB, Lauffenburger DA. The receptor AXL diversifies EGFR signaling and limits the response to EGFR-targeted inhibitors in triple-negative breast cancer cells. Sci Signal. 2013; 6:ra66. [PubMed: 23921085]
16. Lew ED, Oh J, Burrola PG, Lax I, Zagórska A, Través PG, et al. Differential TAM receptor-ligand-phospholipid interactions delimit differential TAM bioactivities. Elife. 2014; 3
17. Meyer AS, Zweemer AJM, Lauffenburger DA. The AXL Receptor is a Sensor of Ligand Spatial Heterogeneity. Cell Syst. 2015; 1:25–36. [PubMed: 26236777]
18. Suzuki J, Denning DP, Imanishi E, Horvitz HR, Nagata S. Xk-related protein 8 and CED-8 promote phosphatidylserine exposure in apoptotic cells. Science. 2013; 341:403–6. [PubMed: 23845944]
19. Nagata S, Suzuki J, Segawa K, Fujii T. Exposure of phosphatidylserine on the cell surface. Cell Death Differ. 2016; 23:952–61. [PubMed: 26891692]
20. Kelleher RJ, Balu-Iyer S, Loyall J, Sacca AJ, Shenoy GN, Peng P, et al. Extracellular Vesicles Present in Human Ovarian Tumor Microenvironments Induce a Phosphatidylserine-Dependent Arrest in the T-cell Signaling Cascade. Cancer Immunol Res. 2015; 3:1269–78. [PubMed: 26112921]
21. Riedl S, Rinner B, Asslaber M, Schaider H, Walzer S, Novak A, et al. In search of a novel target - phosphatidylserine exposed by non-apoptotic tumor cells and metastases of malignancies with poor treatment efficacy. Biochim Biophys Acta. 2011; 1808:2638–45. [PubMed: 21810406]
22. Ran FA, Hsu PD, Wright J, Agarwala V, Scott DA, Zhang F. Genome engineering using the CRISPR-Cas9 system. Nat Protoc. 2013; 8:2281–308. [PubMed: 24157548]
23. Kim YE, Chen J, Chan JR, Langen R. Engineering a polarity-sensitive biosensor for time-lapse imaging of apoptotic processes and degeneration. Nat Methods. 2010; 7:67–73. [PubMed: 19966809]
24. Crescitelli R, Lässer C, Szabó TG, Kittel A, Eldh M, Dianzani I, et al. Distinct RNA profiles in subpopulations of extracellular vesicles: apoptotic bodies, microvesicles and exosomes. J Extracell Vesicles. 2013; 2:20677.
25. Dunne PD, McArt DG, Blayney JK, Kalimutho M, Greer S, Wang T, et al. AXL is a key regulator of inherent and chemotherapy-induced invasion and predicts a poor clinical outcome in early-stage colon cancer. Clin Cancer Res. 2014; 20:164–75. [PubMed: 24170546]
26. van den Besselaar AM, Neuteboom J, Meeuwisse-Braun J, Bertina RM. Preparation of lyophilized partial thromboplastin time reagent composed of synthetic phospholipids: usefulness for monitoring heparin therapy. Clin Chem. 1997; 43:1215–22. [PubMed: 9216459]
27. Lee Y, Lee M, Kim S. Gas6 induces cancer cell migration and epithelial-mesenchymal transition through upregulation of MAPK Slug. Biochem Biophys Res Commun. 2013; 434:8–14. [PubMed: 23567973]
28. Han J, Tian R, Yong B, Luo C, Tan P, Shen J, et al. Gas6/Axl mediates tumor cell apoptosis, migration and invasion and predicts the clinical outcome of osteosarcoma patients. Biochem Biophys Res Commun. 2013; 435:493–500. [PubMed: 23684620]
29. Pirmohamed M. Warfarin: almost 60 years old and still causing problems. Br J Clin Pharmacol. 2006; 62:509–11. [PubMed: 17061959]
30. Ryan JJ, Ketcham AS, Wexler H. Warfarin treatment of mice bearing autochthonous tumors: effect on spontaneous metastases. Science. 1968; 162:1493–4. [PubMed: 5700070]
31. Paolino M, Choidas A, Wallner S, Pranjic B, Uribesalgo I, Loeser S, et al. The E3 ligase Cbl-b and TAM receptors regulate cancer metastasis via natural killer cells. Nature. 2014; 507:508–12. [PubMed: 24553136]
32. Gray MJ, Gong J, Hatch MM, Nguyen V, Hughes CC, Hutchins JT, et al. Phosphatidylserine-targeting antibodies augment the anti-tumorigenic activity of anti-PD-1 therapy by enhancing immune activation and downregulating pro-oncogenic factors induced by T-cell checkpoint inhibition in murine triple-negative breast cancers. Breast Cancer Res. 2016; 18:50. [PubMed: 27169467]

33. Kanada M, Bachmann MH, Contag CH. Signaling by Extracellular Vesicles Advances Cancer Hallmarks. Trends in Cancer. 2016; 2:84–94. [PubMed: 28741553]
34. Costa-Silva B, Aiello NM, Ocean AJ, Singh S, Zhang H, Thakur BK, et al. Pancreatic cancer exosomes initiate pre-metastatic niche formation in the liver. Nat Cell Biol. 2015; 17:816–26. [PubMed: 25985394]
35. Melo SA, Sugimoto H, O'Connell JT, Kato N, Villanueva A, Vidal A, et al. Cancer exosomes perform cell-independent microRNA biogenesis and promote tumorigenesis. Cancer Cell. 2014; 26:707–21. [PubMed: 25446899]
36. Moller-Tank S, Maury W. Phosphatidylserine receptors: enhancers of enveloped virus entry and infection. Virology. 2014; 468-470:565–80. [PubMed: 25277499]
37. Zhou Z. New phosphatidylserine receptors: clearance of apoptotic cells and more. Dev Cell. 2007; 13:759–60. [PubMed: 18061557]
38. Keller S, König AK, Marmé F, Runz S, Wolterink S, Koensgen D, Mustea A, et al. Systemic presence and tumor-growth promoting effect of ovarian carcinoma released exosomes. Cancer Lett. 2009; 278:73–81. [PubMed: 19188015]
39. Suzanne M, Steller H. Shaping organisms with apoptosis. Cell Death Differ. 2013; 20:669–75. [PubMed: 23449394]
40. Fogarty CE, Diwanji N, Lindblad JL, Tare M, Amcheslavsky A, Makhijani K, et al. Extracellular Reactive Oxygen Species Drive Apoptosis-Induced Proliferation via Drosophila Macrophages. Curr Biol. 2016; 26:575–84. [PubMed: 26898463]
41. Ford CA, Petrova S, Pound JD, Voss JJ, Melville L, Paterson M, et al. Oncogenic properties of apoptotic tumor cells in aggressive B cell lymphoma. Curr Biol. 2015; 25:577–88. [PubMed: 25702581]
42. Huang Q, Li F, Liu X, Li W, Shi W, Liu FF, et al. Caspase 3-mediated stimulation of tumor cell repopulation during cancer radiotherapy. Nat Med. 2011; 17(7):860–6. [PubMed: 21725296]
43. Obenauf AC, Zou Y, Ji AL, Vanharanta S, Shu W, Shi H, et al. Therapy-induced tumour secretomes promote resistance and tumour progression. Nature. 2015; 520:368–72. [PubMed: 25807485]
44. Myers SH, Brunton VG, Unciti-Broceta A. AXL Inhibitors in Cancer: A Medicinal Chemistry Perspective. J Med Chem. 2016; 59:3593–608. [PubMed: 26555154]
45. Corno C, Gatti L, Lanzi C, Zaffaroni N, Colombo D, Perego P. Role of the Receptor Tyrosine Kinase Axl and its Targeting in Cancer Cells. Curr Med Chem. 2016; 23:1496–512. [PubMed: 27048336]
46. Kariolis MS, Miao YR, Jones DS, Kapur S, Mathews II, Giaccia AJ, et al. An engineered Axl 'decoy receptor' effectively silences the Gas6-Axl signaling axis. Nat Chem Biol. 2014; 10:977–83. [PubMed: 25242553]
47. Antony J, Tan TZ, Kelly Z, Low J, Choolani M, Recchi C, Gabra H, et al. The GAS6-AXL signaling network is a mesenchymal (Mes) molecular subtype-specific therapeutic target for ovarian cancer. Sci Signal. 2016; 9:ra97. [PubMed: 27703030]
48. Tirosh I, Izar B, Prakadan SM, Wadsworth MH, Treacy D, Trombetta JJ, et al. Dissecting the multicellular ecosystem of metastatic melanoma by single-cell RNA-seq. Science. 2016; 352:189–96. [PubMed: 27124452]
49. Birge RB, Boeltz S, Kumar S, Carlson J, Wanderley J, Calianese D, et al. Phosphatidylserine is a global immunosuppressive signal in efferocytosis, infectious disease, and cancer. Cell Death Differ. 2016; 23:962–78. [PubMed: 26915293]

Implications

This study demonstrates that motility behavior of AXL-expressing tumor cells can be elicited by Gas6-bearing apoptotic bodies generated from tumor treatment with therapeutics that produce killing of a portion of the tumor cells present but not all, hence generating potentially problematic invasive and metastatic behavior of the surviving tumor cells.

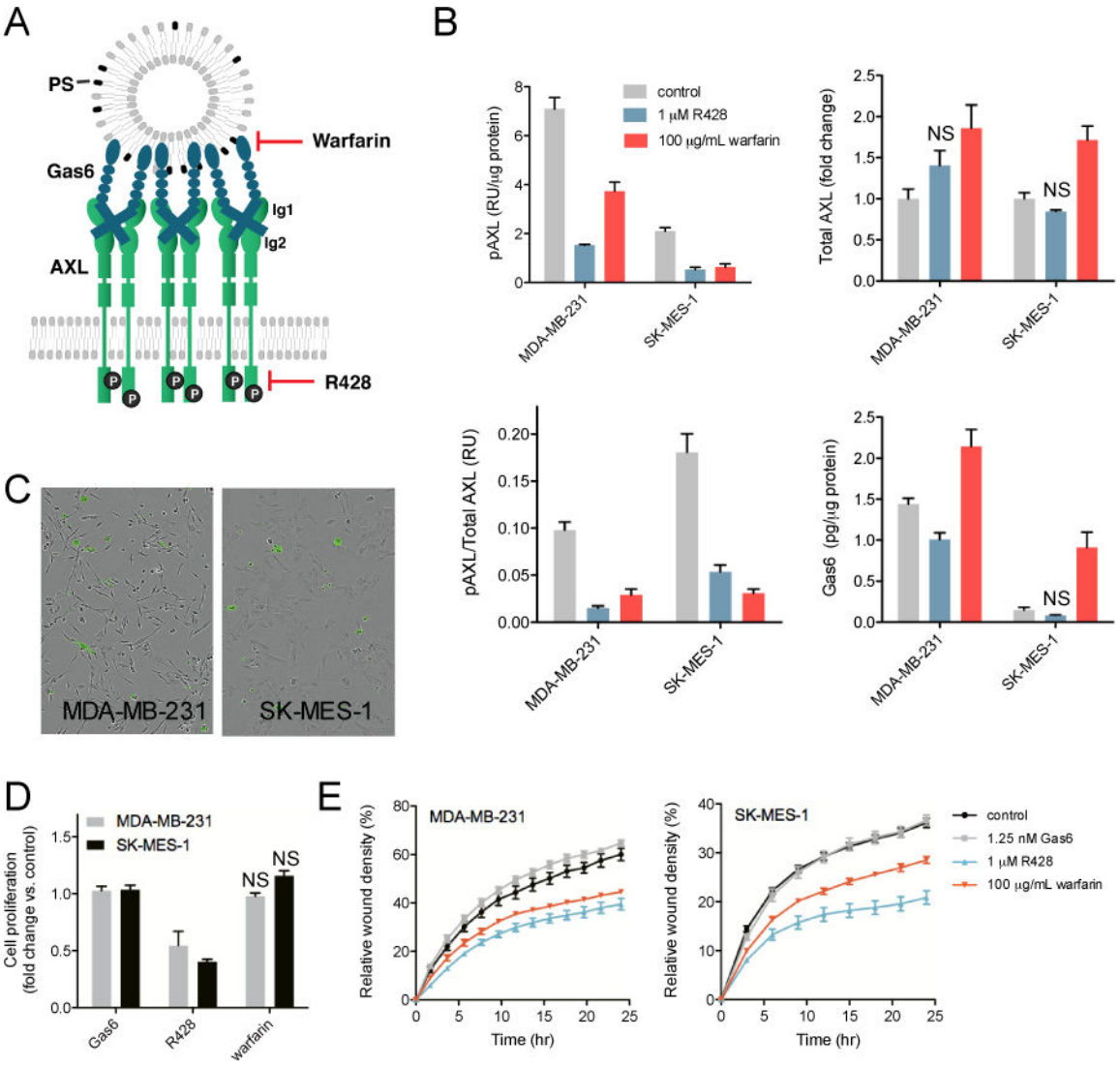

Fig. 1. PS-mediated AXL activation is important for migration

(A) Gas6 binds to PS on extracellular vesicles, driving AXL dimerization and activation. Therefore, two strategies for inhibiting AXL activation are by preventing the Gas6-PS interaction using warfarin, or inhibiting the tyrosine kinase domain with R428. (B) Phosphorylated AXL (pAXL), total AXL and Gas6 levels quantified after 24 hrs of treatment with 1 μM R428 or 100 μg/mL warfarin. Data are means ± SEM of three biological replicates. All measurements are significantly different ($p < 0.05$, Student's *t* test) compared to control, except for bars annotated with NS (not significant). (C) Polarity-sensitive Annexin-V Green binding [22] to exposed PS in MDA-MB-231 (left) and SK-MES-1 (right) cells after 24 hrs of culturing. A green fluorescent signal is only emitted when bound to PS on apoptotic cells. (D) Cell proliferation measured in a Cell Titer Glo assay after 72 hrs of treatment with 1.25 nM Gas6, 1 μM R428 or 100 μg/mL warfarin. Data are means ± SEM of three biological measurements. (E) Cell migration measured in a wound scratch assay after treatment with 1.25 nM Gas6, 1 μM R428 or 100 μg/mL warfarin. The relative wound density, a representation of the cell density (per unit area) in the established

wound area relative to the cell density outside of the wound area, was measured over 24 hrs. A representative graph of one experiment performed in replicates of six is shown.

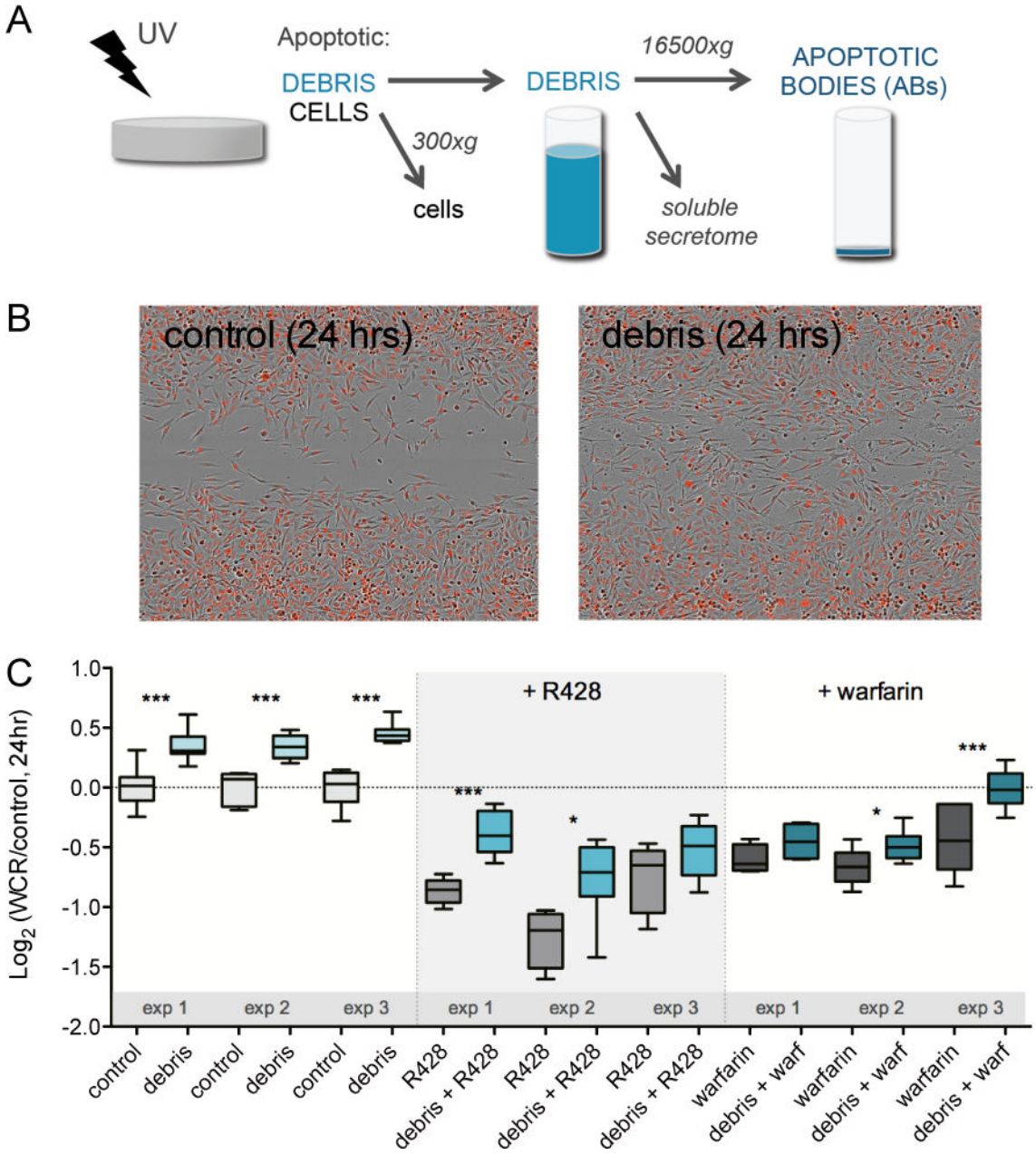

Fig. 2. Apoptotic cell debris induces AXL-dependent cell migration

(A) Preparation and isolation of apoptotic cell debris and apoptotic bodies (ABs) from non-AXL expressing HCC827 lung cancer cells by means of UV irradiation and centrifugation. (B) Representative images of the wound density 24 hrs after scratching a confluent MDA-MB-231-red monolayer, in the absence (left) and the presence of apoptotic cell debris (right). (C) Wound closure rate (WCR) of MDA-MB-231-red cells upon addition of apoptotic cell debris with or without 1 μM R428 or 100 μg/mL warfarin. Data of three independent experiments is presented as Log2 of median with whiskers representing the 5 to 95 percentile of at least eight measurements per condition (*p < 0.05, **p < 0.01, ***p < 0.001, Student's *t* test).

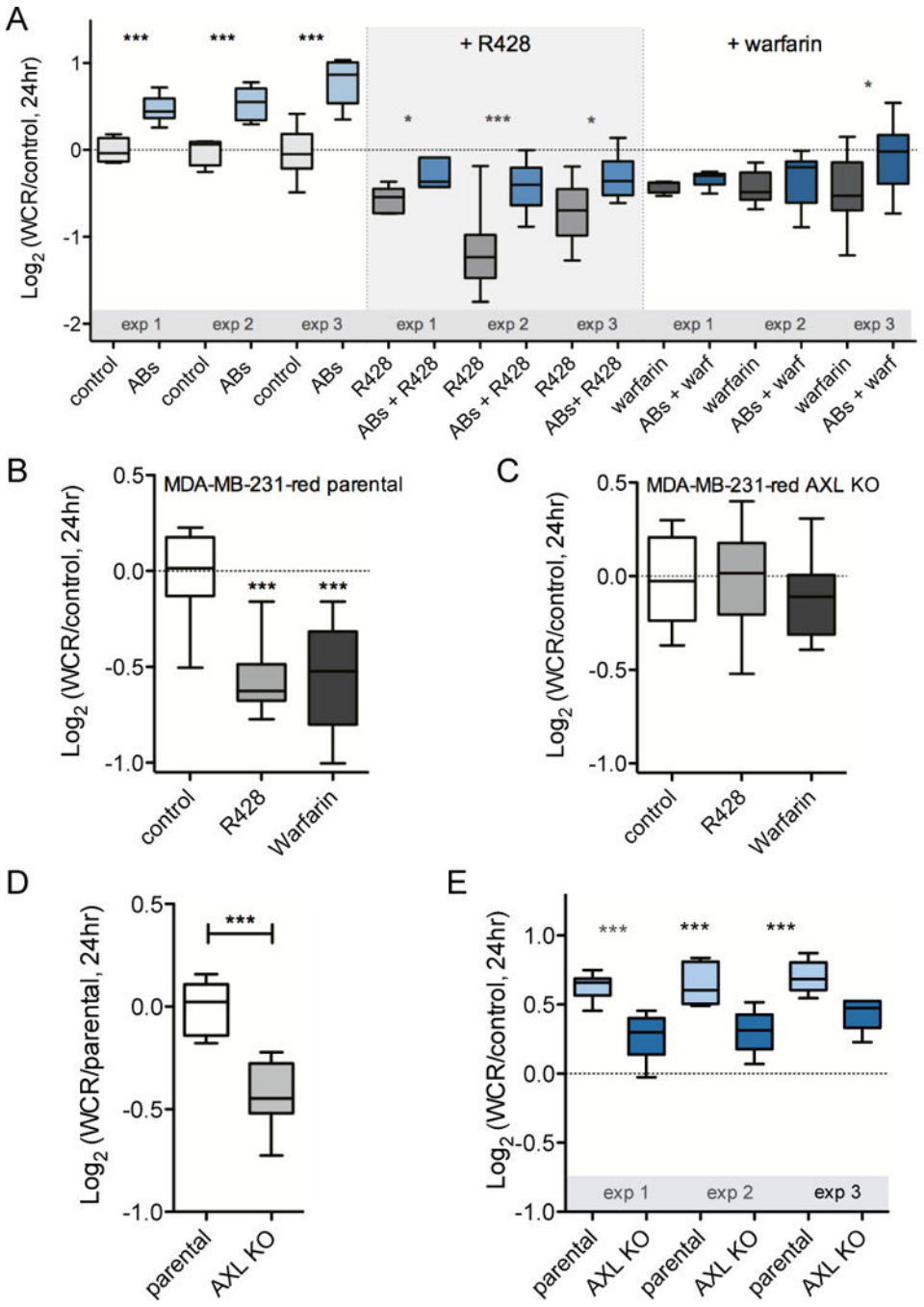

Fig. 3. Apoptotic bodies induce AXL-dependent cell migration

(A) Wound closure rate (WCR) of MDA-MB-231-red cells upon addition of apoptotic bodies (ABs) with or without 1 μM R428 or 100 μg/mL warfarin. Data of three independent experiments is presented as Log2 of median with whiskers representing the 5 to 95 percentile of at least eight measurements per condition (*p < 0.05, **p < 0.01, ***p < 0.001, Student's *t* test). (B+C) Wound closure rate (WCR) of MDA-MB-231-red parental cells (B) and AXL knock out (KO) cells (C) upon addition of 1 μM R428 or 100 μg/mL warfarin. Pooled data of three independent experiments is presented as Log2 of median with whiskers

representing the 5 to 95 percentile. (***$p < 0.001$, Student's *t* test). (D) Wound closure rate (WCR) of MDA-MB-231-red parental cells and AXL knock out (KO) cells. Data is presented as in (B). (E) Wound closure rate (WCR) of MDA-MB-231-red parental cells and AXL knock out cells in the presence of apoptotic bodies (ABs). Data is presented as in (A).

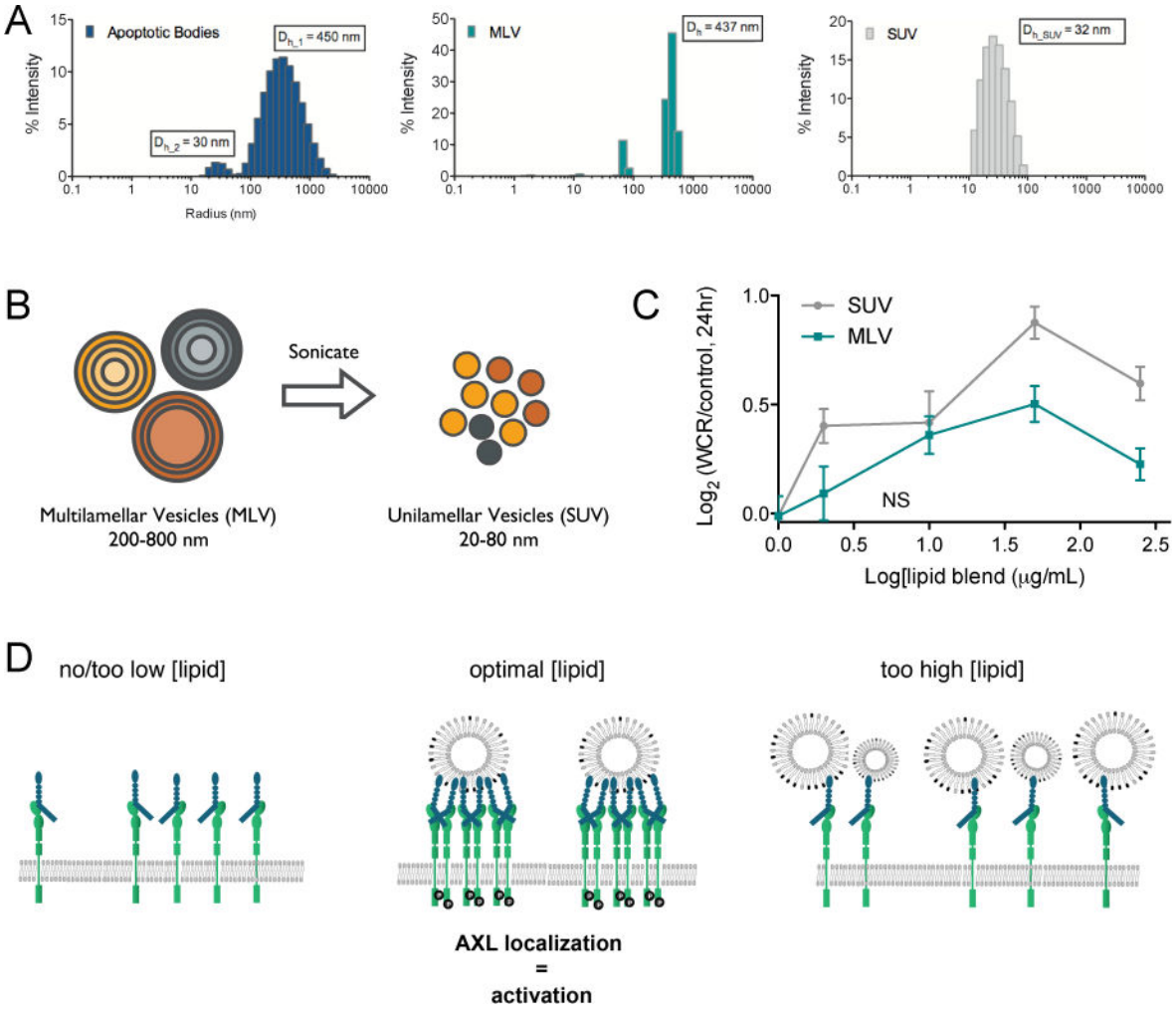

Fig. 4. PS-containing liposomes induce cell migration

(A) Vesicle size distribution detected by dynamic light scattering of apoptotic bodies from HCC827 cells as used in Fig. 2C, small unilamellar vesicles (SUVs) and multilamellar vesicles (MLVs) synthesized with a 5:3:2 w/w lipid blend of DOPE:DOPS:DOPC. The mean hydrodynamic diameter (D_h) of one representative experiment is presented. (B) Schematic representation of multilamellar (MLVs) with several lamellar phase lipid bilayers and sonicated unilamellar vesicles (SUVs) with one lipid bilayer. (C) Wound closure rate (WCR) of MDA-MB-231-red cells upon addition of increasing concentrations of SUVs and MLVs. Data is presented as the Log2 of mean ± SEM of a representative graph of one experiment performed in replicates of six. All measurements are significantly different ($p < 0.05$, Student's *t* test) compared to control, except for the data point annotated with NS (not significant). (D) Model of the biphasic lipid response. AXL localization and activation occurs in the presence of an optimal lipid concentration.

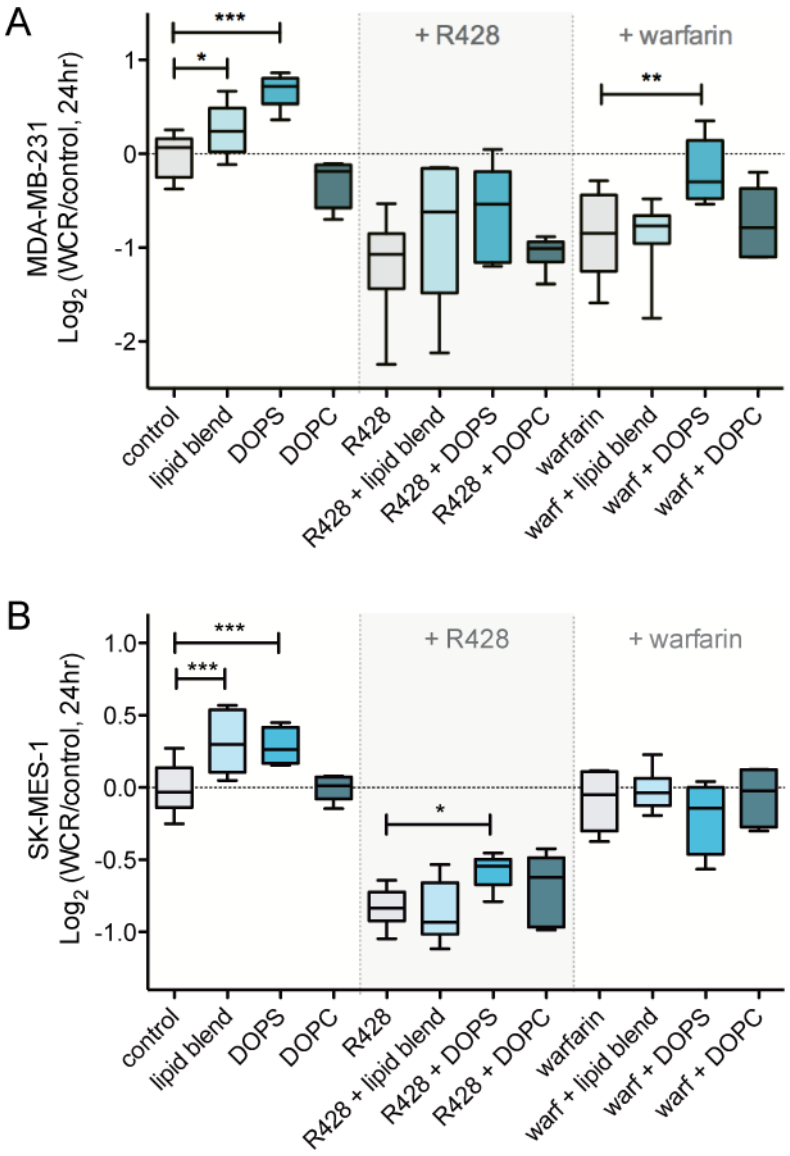

Fig. 5. PS-containing liposomes induce AXL-mediated cell migration in MDA-MB-231 cells (A) and SK-MES-1 cells (B)

Wound closure rates upon addition of DOPS alone, DOPC alone and a 5:3:2 w/w lipid blend of DOPE:DOPS:DOPC in the presence and absence of 1 μM R428 or 100 μg/mL warfarin. All lipids were present at a concentration of 50 μg/mL. Data are presented as Log2 of median with whiskers representing the 5 to 95 percentile of three independent experiments performed in replicates of six (*$p < 0.05$, **$p < 0.01$, ***$p < 0.001$, Student's *t* test).

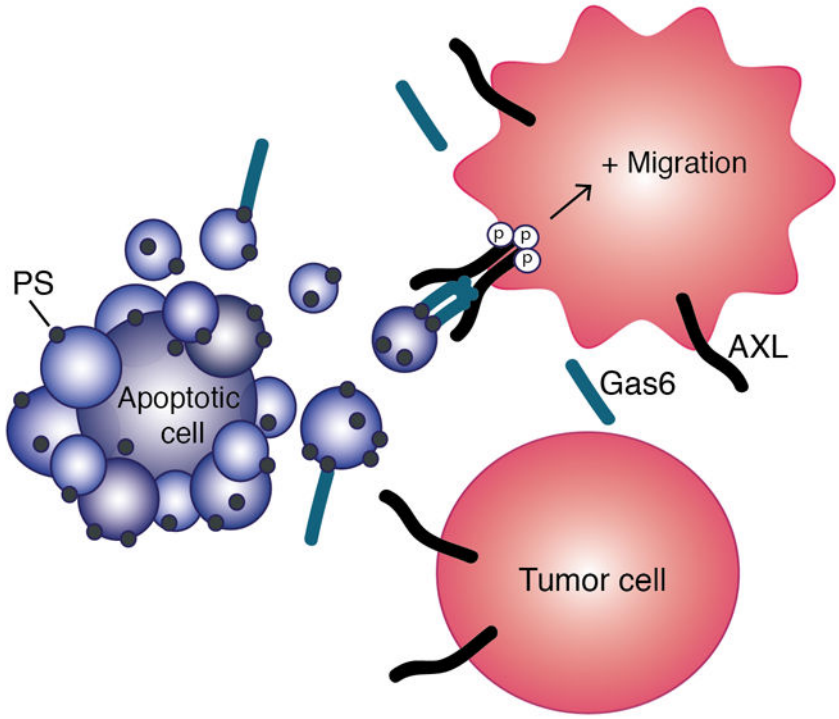

Fig. 6. Model of apoptosis-induced migration upon AXL activation by the PS-Gas6 complex as presented on apoptotic bodies

Surrounding AXL-expressing tumor cells are influenced by bursts in PS exposure generated by surrounding apoptotic cells, leading to increased AXL activation and cell migration.